

Hornbill: A Portable, Touchless, and Battery-Free Electrochemical Bio-tag for Multi-pesticide Detection

Guorong He^{1,3}, Yaxiong Xie² Chao Zheng^{1,3}, Longlong Zhang^{1,4}, Qi Wu^{1,6},
Wenyan Zhang^{1,6}, Dan Xu^{1,3,4*}, Xiaojiang Chen^{1,3,4,5}

¹ Northwest University, Xi'an, China, ² University at Buffalo SUNY, New York, USA

³ Shaanxi International Joint Research Centre for the Battery-Free Internet of Things, China

⁴ Xi'an Advanced Battery-Free Sensing and Computing Technology International Science and Technology Cooperation Base, China

⁵ Internet of Things Research Center, Northwest University, China

⁶ Key Laboratory of Synthetic and Natural Functional Molecule of the Ministry of Education, China

guorong.nwu@gmail.com,yaxiongx@buffalo.edu,{zhengchao,zhanglonglong,wq}@stumail.nwu.edu.cn,
{zhangwy,xudan,xjchen}@nwu.edu.cn

ABSTRACT

Pesticide overuse poses significant risks to human health and environmental integrity. Addressing the limitations of existing approaches, which struggle with the diversity of pesticide compounds, portability issues, and environmental sensitivity, this paper introduces *Hornbill*. A wireless and battery-free electrochemical bio-tag that integrates the advantages of NFC technology with electrochemical biosensors for portable, precise, and touchless multi-pesticide detection. The basic idea of *Hornbill* is comparing the distinct electrochemical responses between a pair of biological receptors and different pesticides to construct a unique set of feature fingerprints to make multi-pesticide sensing feasible. To incorporate this idea within small NFC tags, we reengineer the electrochemical sensor, spanning the antenna to the voltage regulator. Additionally, to improve the system's sensitivity and environmental robustness, we carefully design the electrodes by combining microelectrode technology and materials science. Experiments with 9 different pesticides show that *Hornbill* achieves a mean accuracy of 93% in different concentration environments and its sensitivity and robustness surpass that of commercial electrochemical sensors.

CCS CONCEPTS

- Computer systems organization → Sensor networks;
- Computing methodologies → Feature selection; • Hardware → Wireless integrated network sensors;

KEYWORDS

NFC, Embedded Systems, Electrochemical Measurement, Microelectrode Technology, Pesticide Sensing

*Dan Xu is the corresponding author.

ACM Reference Format:

Guorong He^{1,3}, Yaxiong Xie² Chao Zheng^{1,3}, Longlong Zhang^{1,4}, Qi Wu^{1,6}, and Wenyan Zhang^{1,6}, Dan Xu^{1,3,4*}, Xiaojiang Chen^{1,3,4,5}. 2024. *Hornbill: A Portable, Touchless, and Battery-Free Electrochemical Bio-tag for Multi-pesticide Detection*. In *International Conference On Mobile Computing And Networking (ACM MobiCom '24)*, November 18–November 22, 2024, Washington D.C., DC, USA. ACM, New York, NY, USA, 16 pages. <https://doi.org/10.1145/3636534.3690693>

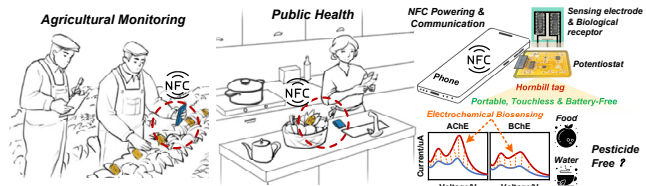


Figure 1: Applications and basic concept of *Hornbill*.

1 INTRODUCTION

Motivation & Problem Statement. Nowadays, global agriculture heavily relies on a variety of pesticides, such as insecticides, herbicides, rodenticides, and fungicides, are extensively employed to mitigate the impact of various pests on crop health [42, 64]. As a result, residues from these pesticides can be identified not only on the surfaces of crops but also in soil, air, and water sources [37, 79].

However, repeated exposure to pesticides is associated with various health issues, including neurological disorders, autism, Alzheimer's, kidney failure, and cancer [39, 40]. Even at low concentrations, pesticide exposure may impede early cognitive development in infants and young children [55]. In addition, some highly toxic pesticides even persist in the soil for an extended duration, exerting detrimental effects on the local sustainable ecosystem [3, 4, 8, 9, 75].

Limitations of Prior Art. Chromatography-based methods [35, 56, 83] are key for analyzing pesticide residues, offering sensitive and reliable results. However, their application is restricted by the need for non-portable lab instruments, valuable equipment, skilled operator requirements, sample pretreatment, and time-consuming processes [81]. For quick field tests, affordable color cards or test papers using Raman spectroscopy [82] are available. Yet, these face performance issues under tough conditions like light, temperature variations, or low concentrations of pesticides.

Recently, electrochemical biosensors have garnered escalating attention owing to their sensitivity and selectivity, fast response, time-saving processes, user-friendly procedures, and low cost [14, 38, 50, 62]. These sensors incorporate three integral components: A biological receptor, a sensing electrode and an electrochemical potentiostat [69], as depicted in Fig. 1. The sensing electrode becomes specific and sensitive through integration with carefully designed biological receptors. The potentiostat will transform the biosignals generated upon the electrode into various forms of electrical signals (voltage, current, resistance). By measuring changes in the sensor's electrical parameters, the properties and concentration of the test substance can be obtained.

However, after numerous trials in real-world deployments, electrochemical biosensor today only finds its use in very specific pesticide detection scenarios [19, 76, 81]. The reasons are as follows: *i) It's unable to cover wide-ranging pesticide types.* According to statistics [37], the current global inventory includes approximately 659 types of pesticides. The high specificity of biological receptors permits the identification of only one or a few classes of pesticides [49, 57, 81]. The simultaneous identification of multiple species of pesticides with different structures and properties is a formidable challenge. *ii) It's vulnerable to environmental changes.* The electrodes in sensors contain biological elements such as enzymes, proteins, antibodies, and nucleic acids. These elements are sensitive to environmental factors such as temperature, humidity, and pH levels, which can affect the sensor's performance [22]. *iii) It's picky for power supply voltage.* The chemical molecules present in pesticides (organophosphates or carbamates) generate electrically active substances upon contact with biological materials. These substances undergo redox reactions under specific external voltage stimulation, thereby generating electrical signals [51]. However, each electrically active substance has its specific redox potential, with some even reaching as high as 0.7-1V [1, 18]. This necessitates the sensor to apply higher voltage across electrodes to meet the redox potential required for reactions. As a result, sensors often require bulky batteries [87] or wired solutions [65], increasing the overall system volume and weight. Moreover, wired solutions need direct contact between equipment and the tested crops, soil, or water, thereby

elevating users' exposure to pesticides. This poses a particular concern for professionals engaged in frequent pesticide testing, including pesticide and water quality monitoring personnel, as well as researchers in related fields.

Proposed Solution. Near-field Communication (NFC) technology is widely applied as a user interface for tangible and social computing systems (e.g., smartphones and smart-watches), which provide a reliable and non-contact channel for bi-directional data communication between battery-less devices (e.g. tags, sensors) [20, 84, 88]. The high energy efficiency of NFC (15mW output power per chip) can support the power supply required for most sensing applications [11, 48]. *Is there a vision where ordinary citizens or researchers can achieve portable, precise, and touchless multi-pesticide detection anytime, anywhere through NFC technology?*

This work presents *Hornbill*¹, a wireless and battery-free sensing system based on cheap NFC tags for multi-pesticide residue detection, as shown in Fig. 1. At a high level, we integrate the advantages of backscatter technology with electrochemical biosensors. *Hornbill* uses thin NFC tags as an energy source and communication device for electrochemical biosensors. After the *Hornbill* tag comes into contact with the pesticide-containing test sample, molecular-level electrochemical signals from the test sample are continuously and selectively gathered by the sensing electrode, carried through the low-noise, reusable sensor-electronics physical interface acquired by the electronics, and wirelessly relayed through NFC to the user's mobile app for visualization and analysis. The entire operation is thus NFC-controlled by the accompanying mobile app.

To design such a practical bioelectrochemical tag that functions robustly on a battery-free, completely NFC-powered system, we have the following design goals.

- *Broad-spectrum pesticide detection:* The system must be versatile enough to handle the diverse chemical structures and action mechanisms of pesticides.
- *Sufficient potential for electrochemical reactions:* Even with NFC powering, applying a voltage of nearly 1V to the electrode poses challenges. An effective voltage regulation scheme is necessary to ensure that the bioelectrode maintains a high enough voltage while other components of the sensor function properly.
- *Superior sensitivity for low-concentration pesticide:* For the electrode, detecting subtle changes in pesticide molecules is crucial and demands extremely high sensitivity.
- *Environmental robustness:* The sensor must possess a prolonged lifespan and maintain reliable operation in challenging environments.

¹A bird species living in tropical and subtropical regions of Africa, Asia, and Melanesia. According to Malaysian folklore, the hornbill's beak changes color upon contact with toxic substances.

For the first goal, *Hornbill* achieves the detection of multiple pesticides by comparing the distinct interactions between a pair of biological receptors and different pesticides. Specifically, various pesticide molecules induce distinct inhibitory effects on cholinesterase proteins. This divergence arises from the different binding positions of functional groups from various pesticide molecules on cholinesterase. The disparities in these binding sites influence the affinity and stability of the interaction between pesticides and cholinesterase. Consequently, under identical voltage stimulation, varying peak potentials are generated (Fig. 3). By contrasting the differential impacts of various pesticides on the same pair of cholinesterase proteins, *Hornbill* makes broad-spectrum pesticide residue detection feasible.

To achieve our second objective, we've developed a voltage regulator integrated with an electrochemical sensor. Our key idea is to exploit a charge pump as the voltage conversion circuit that raises voltage through periodic charge transfer. Specifically, we replaced the single (3.3V) voltage output by the NFC chip with negative voltage (-3.3V) through the charge pump circuit and connected it as an additional voltage source to the amplifier end to replace the single-supply power supply method. In this manner, the system has transitioned from a single power supply to a dual power supply, effectively doubling the power supply voltage to 6.6V. This voltage satisfies the redox potential necessary for the electrochemical reaction of the majority of pesticide molecules.

For the third goal, we present the development of target-sensitive, cholinesterase-embedded interdigitated microelectrodes (IMEs). Inspired by microelectrode arrays [28, 31], our design incorporates an array of microband electrodes, where alternating microbands are interconnected to form interlocking electrode fingers. This configuration offers superior sensitivity compared to traditional macro-sized electrodes. The close proximity of micro-anodes and cathodes enhances the cycling efficiency of small ionic species [41], accelerating the diffusion of pesticide molecules across the electrodes and increasing the current at redox peaks, thereby improving detection efficiency.

As for the last goal, we use a nanocomposite to cover our sensing layer to shield biological receptors from environmental influences. The nanocomposite consists of *zinc imidazolate metal-organic framework-8* (ZIF-8) blended in the *chitosan* (CS). The robust thermochemical stability exhibited by ZIF-8 positions them as an optimal choice for drug delivery and biomedical applications [30]. CS is commercially produced from crustacean exoskeletons (e.g., crabs and shrimp) and fungal cell walls. It is commonly employed as a bioadhesive in biomedical applications [23]. Specifically, we fabricated an 'armor' composed of ZIF-8 and CS, which wrapped around the cholinesterase, utilizing the environmental stability of ZIF-8 to protect the biological receptors.

Contributions. To summarize, this paper makes the following contributions: **(i)** We present *Hornbill*, a wireless and battery-free pesticide detection system that integrates the advantages of Near-field Communication technology with electrochemical biosensors. *Hornbill* enables portable, touchless, and robust multi-pesticide detection. **(ii)** We propose novel designs spanning across hardware and software to address various challenges including limited voltage range, insensitive electrode structure, vulnerable biological receptors, and confusing signal features. **(iii)** We develop *Hornbill* tags, each costing under \$9, and deploy them in real-world environments. Extensive testing with a commercial Android phone equipped with NFC was conducted and compared to results from a \$5400 CHI620E electrochemistry workstation. Testing across nine pesticides demonstrates that *Hornbill* enables accurate, touchless, and robust multi-pesticide detection, exhibiting superior sensitivity and durability compared to previous studies.

2 BACKGROUND AND MOTIVATION

The broad-spectrum pesticide sensor we designed originates from the principle of electrochemical biosensing. We expound upon this concept and present our design in the forthcoming sections.

2.1 Three-Electrode Measurement.

Three-electrode based electrochemical measurement is the most widely used method to identify and qualify the concentration of materials. A three-electrode, as indicated by its name, consists of three electrodes, the *working electrode* (WE), the *reference electrode* (RE), and the *counter electrode* (CE), just shown in Figure 2(a). Within an electrolytic cell housing the materials to be measured, or the *reactant*, the three electrodes play distinct roles: the WE operates as the anode, carrying a positive charge; while the CE functions as the cathode, maintaining a positive charge. Together, they establish a circuit during the electrochemical process. The RE serves a critical function by providing a stable and known potential, acting as a reliable reference point against which the potential of the WE can be measured accurately.

During the measurement process, the potential difference between the RE and WE initiates the oxidation of the reactant, leading to the generation of freely moving electrons. Due to the extremely high resistance of the RE, the majority of these electrons flow towards the CE, establishing a current I_f between the WE and CE. Consequently, monitoring the current flowing between the WE and CE allows us to infer the intensity of the oxidation process. The intensity of the oxidation depends on two factors: the type of material or reactant and the potential difference V_{con} between WE

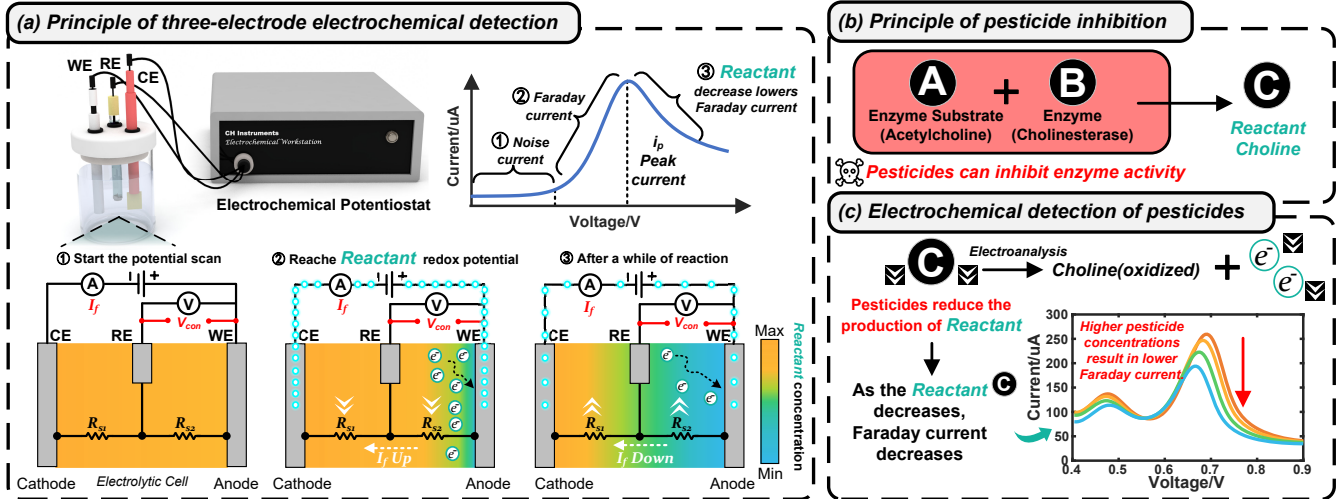


Figure 2: Schematic diagram of pesticide detection by electrochemical biosensor. (a) Basic principle of three-electrode electrochemical detection; (b) Basic principle of pesticide inhibition; (c) Electrochemical measurements are used for pesticide detection.

and RE. Generally, when the potential V_{con} aligns with the reactant's redox potential, the intensity is maximized.

To identify the type of reactant, we leverage a *potentiostat* to sweep across a range of potentials V_{con} , starting from zero. When the V_{con} approaches the reactant's redox potential, we observe a notable increase in current I_f , commonly referred to as Faraday current (the electric current generated by the reduction or oxidation of some chemical substance at an electrode), as depicted in Figure 2(a). However, once the potential surpasses the redox potential, the resulting current diminishes due to two primary factors: the deviation from the redox potential and the reduction in reactant concentration. Upon completing the scanning process, we acquire a spectrum of the reactant, detailing the relationship between the I_f and V_{con} . The shape of this spectrum serves as a distinctive fingerprint characterizing the reactant, allowing for its identification.

2.2 Pesticide Detection

We exploit the interaction between *Acetylcholinesterase* **A** and *Cholinesterase* **B** enzymes for pesticide detection. Illustrated in Figure 2(b), this reaction yields *Choline* **C**, serving as the reactant in the three-electrode setup. Notably, this reaction exhibits high sensitivity to pesticides; even minute concentrations of pesticides can significantly impact the reaction intensity and consequently alter the Choline concentration. Hence, we employ the three-electrode configuration to measure the Choline concentration, enabling the detection and quantification of pesticides. Specifically, elevated pesticide levels correspond to reduced peak Faraday current. Nonetheless, the overall spectrum retains its characteristic shape, as depicted in Figure 2(c).

Multi-pesticide Sensing Principle To cope with the above challenge, our insight is to leverage the differential inhibitory responses of two enzymes, AChE and BChE, towards various pesticides. Specifically, Fig. 3 plots the electrochemical response curves of two enzymes to pesticide *Acephate* with concentrations ranging from 10^{-7} - 10^{-15} mol/L. It is not difficult to observe that compared to AChE, the current inhibition by different concentrations of *Acephate* on BChE is more pronounced (a faster decline in the Faraday current peak), which means that *Acephate* tends to inhibit BChE more than AChE. By leveraging the complementary nature of AChE and BChE, which exhibit different sensitivities and inhibitory kinetics towards pesticides, we can achieve a broad spectrum of pesticide detection.

However, the Faraday current from choline depends on applying high electrical stimulation to the electrodes (redox potential is about 0.7-0.8V). Typically, creating high-potential stimulation requires large batteries or wired devices, which are not portable or safe enough for many applications [33].

2.3 NFC Power & Communication

To bypass the constraints of conventional sensing systems, we've integrated the emerging NFC technology, aiming to propose a pesticide sensing method that operates without wired connections or batteries. As shown in Fig. 4, the NFC reader transmits power and operational commands to the tag through the induction coil, keeping track of load variations as the tag adjusts them. The tag's antenna picks up the energy and sends the requested information back to the reader within a proximity of centimeters through Amplitude Shift Keying (ASK) or Frequency Shift Keying (FSK) modulation at a frequency of 13.56 MHz. Choosing NFC as the channel

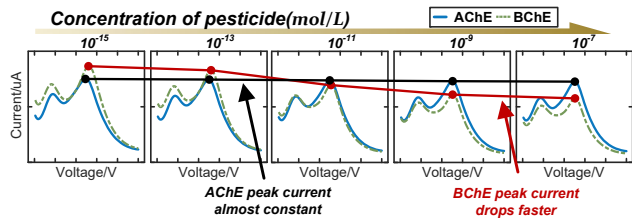


Figure 3: The current inhibition by different concentrations of pesticide *Acephate* on AChE and BChE.

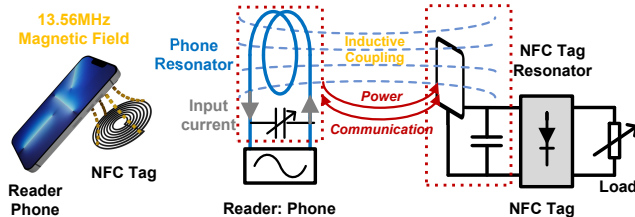


Figure 4: The magnetic coupling between the NFC-enabled phone and a NFC tag.

for power supply and communication brings the following direct advantages.

- NFC offers an unmatched power transfer efficiency compared to other far-field signals [46]. Due to the basic principle behind the electrochemical reactions, a certain amount of electrical energy is required to overcome activation barriers (more than redox potential). In addition, the sensor itself also needs MCU, ADC/DAC, antenna, etc., for control, data acquisition and transmission, which contributes to the system's overall energy consumption (23.8mW [85]). Thanks to the inductive coupling effect, even affordable commercial NFC chips (\$1) can deliver an output power of at least 15mW [71], with some specialized chips reaching up to 200mW [84], showcasing their potential to meet the energy demands of such sensor systems efficiently.

- NFC technology enjoys widespread application across the smart device market, with 60% of smartphones globally being NFC-compatible in 2021 [20]. Integrating an NFC module into an electrochemical biosensor allows smartphones to wirelessly control it through antenna coupling, removing the need for wires or batteries and enabling portable, touchless pesticide detection. Furthermore, the variety of NFC's operating modes (peer-to-peer, reader/writer, and card emulation [68]) along with its multiplexed protocols (ISO 15693 and ISO 14443 [88]), allows for tags to be adaptively used in different pesticide detection scenarios.

3 HORNBILL DESIGN

This section outlines the design of *Hornbill*, starting with an overview, followed by detailed introductions of each module.

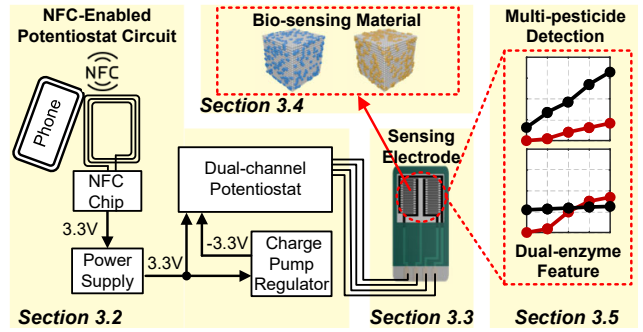


Figure 5: The organization of *Hornbill*.

3.1 System Overview

The system architecture of *Hornbill* is shown in Fig. 5, which contains the following four pivotal modules.

NFC-Enabled Potentiostat Design. Our system is built on a tiny NFC tag and incorporates a dual-channel potentiostat, enabling simultaneous measurement of electrical signals from two biological receptors. To meet the stringent potential requirements of the electrochemical reaction, we enhance the potentiostat with a charge pump regulator, ensuring stable electrochemical detection under NFC activation.

Electrode Design. In addition, we design a sensing electrode with a dual-channel interfinger microstructure to increase the accuracy of pesticide detection in the system.

Material Design. Then, we employ a porous nanomaterial to encapsulate our biological receptors, enhancing the system's environmental robustness and extending its lifespan.

Feature Design. Finally, by analyzing the differences between two enzymatic electrochemical curves, we construct an effective biometric fingerprint, which is then utilized for the classification of multiple pesticides.

3.2 NFC-Enabled Potentiostat Design

3.2.1 Challenge in NFC-Enabled Potentiostat. To understand the voltage supply challenges in bringing the electrochemical biosensor to the NFC tag, let us first understand the basic potentiostat circuit, shown in Fig. 6. The core of the potentiostat is composed of a control amplifier and a trans-impedance amplifier. The control amplifier ensures the potential difference (V_{cell}) between the working and reference electrodes is maintained, triggering the electrochemical reactions. Meanwhile, the trans-impedance amplifier converts the current detected (I_f) into a measurable voltage signal ($V_{out} = I_f \times R_m$).

However, this straightforward approach cannot be directly applied to pesticide molecule detection. The reason can be better explained with the following example. As introduced in Sec. 2, electrochemical detection relies on the redox reaction of electroactive substances to identify their composition. In Choline-based C_2 reactions, the typical redox potential is

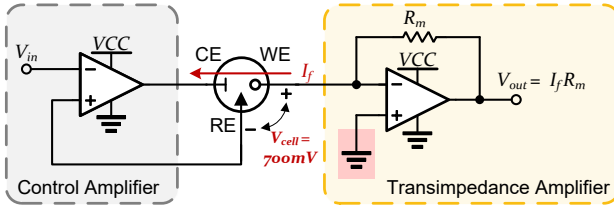


Figure 6: A standard potentiostat circuit.

around 700-800mV [2], relative to a standard RE. In this case, the potential of RE must be maintained at approximately 700mV lower than that of WE to ensure the redox reaction proceeds effectively. However, it's impossible with a single positive supply because WE is held at the lowest potential in the circuit, which is the ground potential.

A feasible approach is to adjust the bias voltage V_{bias} at the non-inverting input of the trans-impedance amplifier to match the specific needs of the reaction, as illustrated in Fig. 7. This presents another issue where the measured voltage at the output of the trans-impedance amplifier V_{out} is no longer referenced to ground.

$$V_{out} = I_f R_m + V_{bias} \quad (1)$$

Since the V_{bias} is typically supplied directly by the system's NFC chip or DAC module, it is prone to environmental interference and thermal noise from the device [21, 44], which may affect the stability and accuracy of measured voltages.

In addition, determining a suitable bias potential can be quite laborious. Based on the equivalent circuit in Fig. 7, if the V_{bias} is set too small, the headroom for the voltage swing at CE (available voltage range of CE) will be insufficient to cover the voltage drop caused by Faraday current [1]. Just like the water pressure at the end of the pipe is lower than the water pressure at the front of the pipe, the current causes a voltage drop as it passes through the circuit resistance. The voltage drop at CE can be expressed as:

$$\Delta V_{ce} = V_{re} - V_{ce} = \frac{(R_{s1} + R_{ce})(V_{we} - V_{re})}{R_{s2} + R_{we}} \quad (2)$$

where R_{we} and R_{ce} represent the charge-transfer resistances of the CE and WE, while R_{s1} and R_{s2} denote the solution resistance between RE&CE, and RE&WE, respectively. C_{ce} and C_{we} are the double-layer capacitances formed between electrodes and solution, minimally impact the redox current and are often disregarded [53]. V_{ce} , V_{re} and V_{we} represent the potentials applied on the three electrodes.

Because the system uses a single power source, the potential at CE must exceed the reference ground. Thus, V_{bias} must satisfy the following equation to keep sufficient available headroom on the CE to handle the voltage drop induced by the Faraday current.

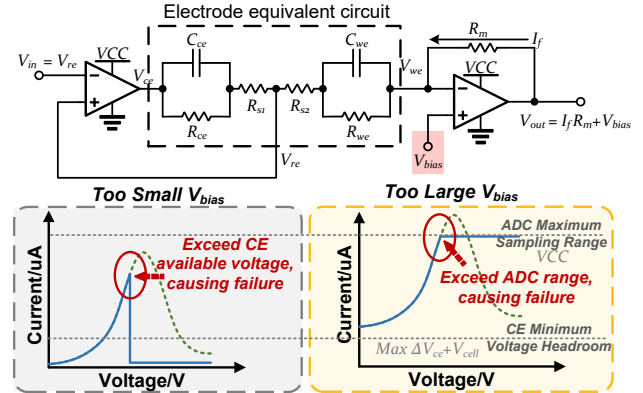


Figure 7: Single voltage supply potentiostat based on bias voltage approach and issues encountered during bias voltage configuration.

$$V_{bias} > V_{cell} + \Delta V_{ce \max} = V_{cell} + \frac{(R_{s1} + R_{ce}) V_{cell}}{R_{s2} + R_{we}} \quad (3)$$

If the V_{bias} is too large, the elevated potential will shrink the sampling range of the system ADC module. Because the ADC sampling range ΔV_{adc} depends on the supply voltage VCC harvested from the NFC tag, which can be modeled as:

$$\Delta V_{adc} = VCC - V_{out} = VCC - I_f R_m - V_{bias} \quad (4)$$

Obviously, without knowing the reaction current (I_f), a too high V_{bias} setting causes ADC sampling easily to go beyond its limit, as shown in Fig. 7). **Note:** Limited by the sampling accuracy of the ADC, directly reducing R_m will lead to inaccuracies in measuring microampere-level currents.

3.2.2 Dual-channel Potentiostat with Dual Voltage Supply. To ensure an adequate potential difference for the sensor's response, while simultaneously benefiting from the stability that comes with the reference grounding, we must bring down the potentials at RE and CE to be lower than ground level. On this basis, Hornbill presents a simple design for a dual-voltage potentiostat, incorporating charge pump circuits.

Fig. 8 details our design of the dual-channel potentiostat circuit. We use a regulator made of charge pump circuits to convert the voltage output from the NFC chip into negative voltage, and then connect it as the voltage source to the other end of the amplifier. The charge pump achieves negative voltage through a meticulously controlled series of charge transfers among capacitors, leveraging the switching capabilities of transistors or diodes [61]. The operation can be broken down into several key phases:

Charge Accumulation. Initially, a capacitor, often referred to as the 'flying capacitor' C_1 is charged to the input voltage during the first half of each cycle (switches $S_1 \& S_3$ close and $S_2 \& S_4$ open). This charging is facilitated by connecting the

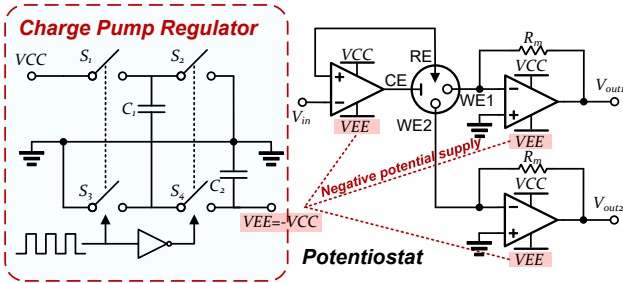


Figure 8: The dual-channel potentiostat with charge pump regulator.

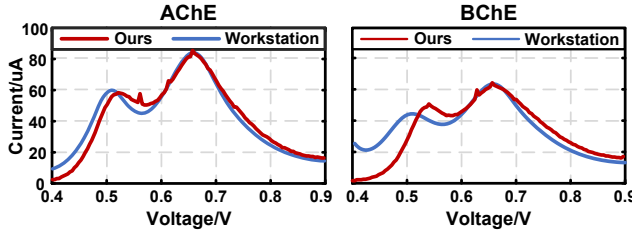


Figure 9: Comparison of I-V curves between our potentiostat and workstation (Analyte: Glyphosate).

capacitor directly across the positive voltage source through a controlled switch.

Voltage Inversion. In the subsequent half cycle, switches $S_2 \& S_4$ close and $S_1 \& S_3$ open, the flying capacitor is disconnected from the input source and reconnected in a configuration that inverts its voltage relative to the ground. This is typically achieved by switching the connections so that the previously grounded side of the capacitor is now connected to the load, and the other side is connected to the ground, effectively inverting the voltage across it ($VEE = -VCC$).

We opted for charge pump as our system's voltage regulator mainly for the following reasons: *Firstly, superior efficiency at low inputs.* Charge pump could maintain a power conversion efficiency of about 90–95% when loaded up to a few milliamps. Conversely, the efficiency of alternatives like Buck converters [70] can fall significantly under some loads, often below 72%. *Secondly, minimal noise.* Since NFC antennas are sensitive to magnetic field changes, charge pumps are advantageous here because of their inductor-less design. The absence of inductors leads to cleaner power delivery, which is critical for the NFC tag's integrity and reliability compared to other inductive-based regulators [43].

To prove the effectiveness of *Hornbill* in NFC tags, we compare it with a dedicated electrochemical workstation (CH Instruments, 620E), focusing on its performance against the pesticide *Glyphosate*. Figure 9 presents the electrochemical response curves of two sensors. Despite minor fluctuations in the current curves caused by noise, our potentiostat accurately captures the complete redox current of reactants.

3.3 Highly-Sensitive Electrode

Another challenge in pesticide sensing is the limited sensitivity of sensor electrodes to low pesticide concentrations. In practice, low-concentration pesticides induce only minimal current changes, typically in the microampere (μA) range [80]. This slight variation makes it difficult for sensors to distinguish these changes from the baseline signal. To enhance detection performance at low pesticide concentrations, it is essential to optimize electrode design to maximize sensor sensitivity.

Electrode Sensitivity Definition. In electrochemistry, Sensitivity s refers to the ability of an electrochemical device to detect changes in the concentration of a measured substance, usually defined as the ratio of the detected peak current Δi_p to the change in analyte concentration ΔM .

$$s = \frac{\Delta i_p}{\Delta M} \quad (5)$$

The peak current i_p is influenced by the interface between the solid electrode and the solution containing the electroactive substance. According to the Cottrell equation [5], the response of its generated peak current i_p over time can be modeled as:

$$i_p(t) = \frac{nFAD^{1/2}M_O}{\pi^{1/2}t^{1/2}} \quad (6)$$

Here, n is the number of transferred electrons, A is the electrode area, and M_O is the concentration profile of the electroactive species near the electrode. F and D are Faraday constant and solution diffusion coefficient, respectively. To boost the peak current, it's necessary to either enlarge the electrode area A or improve the concentration profile M_O near the electrode. Although expanding the electrode's area can boost sensitivity, it also increases background noise, costs, and reduces convenience due to the larger size.

Electrode Design. Inspired by microelectrode technology in neuroscience [41, 58], we make a structural modification to the sensing electrode, aiming to boost its sensitivity by refining the concentration profile M_O , as shown in Fig. 10(a). Specifically, our electrode consists of two pairs of micro-scale, comb-like electrode structures, wherein the 'fingers' of the counter electrode are intricately interwoven between the fingers of the dual working electrodes. Additionally, a reference electrode, mirroring the same micro-scale architecture, is positioned below the two working electrodes.

Contrary to the traditional macroelectrodes (Fig. 10(a), 5 mm diameter), the structure of micrometer-scale interdigitated array results in a significantly higher peak current without increasing the electrode surface area. All of this can be attributed to the different diffusion behavior of the solution on the electrodes.

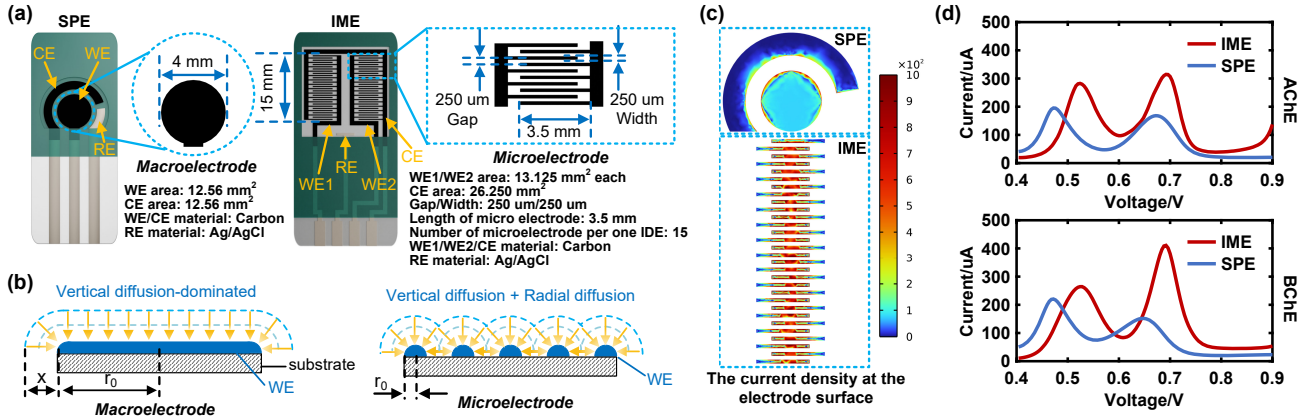


Figure 10: Electrode structure and experimental results. (a) Structural comparison between our electrodes and conventional screen-printed electrodes. (b) Diffusion effects of solutes in macrostructures and microstructures. (c) COMSOL Simulation Current Density. (d) I-V curves of Glyphosate pesticides measured with different electrodes.

Diffusion Equations and Current Responses. For a molecule freely diffusing in solutions, the mean-squared distance traveled x^2 in time can be expressed as $x^2 = 2Dt$. Because the diffusion coefficient of aqueous solution at normal temperature is only $(0.1\text{--}10)\times 10^{-9}\text{ m}^2/\text{s}$, the estimated diffusion distance moves by an average of 10 to $1000\mu\text{m}$.

When the electrode size r_0 is much larger than the distance x of the substance, the diffusion of the analyte is primarily one-dimensional, that is, a straight line movement from the solution volume to the electrode surface (as shown in Fig. 11(b) Macro-sized electrode). This mode of diffusion results in a limited rate of mass transfer, especially after the reaction has proceeded for some time and the analytes near the electrode surface have been depleted, further slowing down the diffusion rate. When the electrode size r_0 is comparable to or smaller than the diffusion distance x , substances in the solution will diffuse not only in a linear path towards the electrode surface but also radially around the electrode in a hemispherical manner (see Fig. 10(b) Micro-sized electrode). Thanks to this combined radial and planar diffusion mode, the mass transfer efficiency on microelectrode is higher. Without the need for stirring, a more uniform concentration distribution can be maintained through natural convection and diffusion.

According to Fick's laws [5], the radial diffusion effect on a micro-sized electrode can increase the concentration profile M_O of electroactive substances around the electrode.

$$M_O = M_O^* \left(1 - \frac{r_0}{x}\right) \quad (7)$$

where M_O^* represents the average concentration of the entire solution environment. It can be seen that when the electrode size decreases, the concentration profile M_O around the electrode is larger, and the peak current i_p is also higher.

To verify the performance of our electrodes, we conduct COMSOL simulations and real-world pesticide detection experiments, comparing them with a macro-sized Screen Printing Electrode (SPE). **Note:** Since our system involves the joint detection of pesticides with two enzymes, we need to design the electrode with two working electrodes, WE1 and WE2. To ensure fairness, here we only use the part of WE1 to ensure that the area is almost identical to that of the traditional electrode. Also, we manufacture two types of electrodes using the same fabrication process (screen printing) and materials (carbon). The specific design parameters are shown in Fig. 10(a). Through the secondary current interface of the COMSOL electrochemistry module [17], we simulate the effects of different electrode structures on current density (Fig. 10(c)), it becomes clear that the IME we've designed showcases a higher current density on their surface area compared to macro-sized electrodes of identical area. Furthermore, from the real-world pesticide detection I-V curve diagrams (Fig. 10(d)), it is evident that for the same concentration (10^{-15} mol/L) of glyphosate pesticide, our microelectrode design captures a larger peak current. These indicate that our electrodes are notably more sensitive, despite slight peak shifts due to differences in electrode structure.

3.4 Environmental Robustness Boost

Considering that enzyme typically has a short effective period at room temperature (4-5 days [10]) and is vulnerable to external influences, this part outlines the safeguarding measures we adopt to fortify the sensor's biological receptor, ensuring its durability and functionality in demanding environments.

Protective Film Made of Porous Materials. We create a protective film for our biological receptor using porous

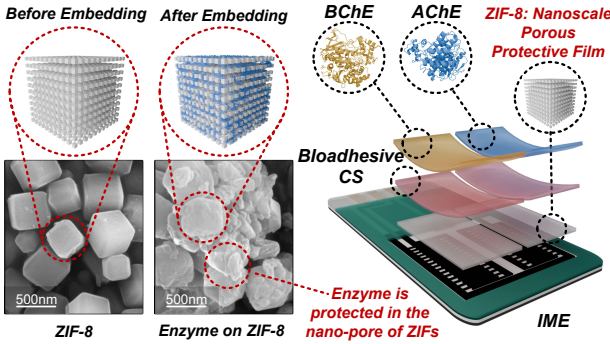


Figure 11: The principle of enzyme protection by ZIF-8 and morphological characterization under SEM.

nanomaterials, safeguarding the enzymes from external damage. ZIF-8, a Zinc Imidazolate metal-organic Framework, is a biocompatible and stable porous crystalline material, ideal for biopharmaceutical applications due to its protective qualities [30, 45]. ZIF-8’s small pores selectively block most harmful molecules, providing enzymes with molecular-level defense. Its unique structure, featuring a cubic void made mainly of zinc, protects the enclosed enzymes from chemical and thermal damage. Importantly, ZIF-8’s biocompatibility ensures it can safely degrade within the body, making it safer for users [29, 86].

Specifically, as shown in Fig. 11, we first mix the ZIF-8 powder into a loose composition, stir it thoroughly, and then apply it to the electrode surface. Subsequently, due to the possible leaching of cholinesterase **B**, we choose chitosan (CS), a bioadhesive with good biocompatibility, as an intermediate layer to ensure the tight connection between ZIF-8 and enzymes. Finally, cholinesterase **B** is added to the mixed layer of ZIF-8 and CS, and through intermolecular Van der Waals forces and pore entrapment [27], cholinesterase **B** is tightly embedded in the pores of ZIF-8. The surface morphology of the material is characterized using Scanning Electron Microscopy (SEM), with the results showcased in Fig. 11. Electron microscopic analysis reveals that the enzymes are closely embedded in the nano-scale pores of ZIF by CS.

3.5 Multi-pesticide Detection

After the above steps, we obtain the reactant’s valid Faraday currents from an NFC tag. To improve the accuracy and reliability of pesticide detection, we create a unique set of features from the I-V curves of two enzymes for representing multiple pesticides.

As shown in Fig. 12, the first step in our method is to extract the Faraday current peaks from the I-V curves for both enzymes. These peak values represent the electrochemical activity induced by the interaction between the enzymes and the pesticides, serving as a critical marker for distinguishing between different pesticide types. To ensure the consistency

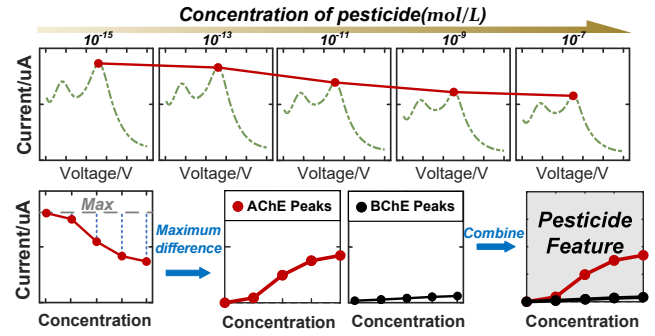


Figure 12: Dual-enzyme feature construction.

of the data set and eliminate noise effects, we use a simple linear difference [34] for data alignment. Specifically, we subtract the maximum value within the dataset from each peak value. This method effectively minimizes the disparities among the samples, ensuring that our analysis focuses on the inherent differences in enzyme-pesticide interactions rather than experimental variances.

Following this differentiation, we proceed to amalgamate the differentiated peak values from both enzymes at various concentrations. This combination of electrochemical responses crafts a comprehensive electrochemical profile for each pesticide, encapsulating the nuanced ways in which different pesticides interact with each enzyme. The resulting data matrix—comprising combined, normalized peak values for multiple pesticides across a range of concentrations—forms the basis of our dual enzyme feature.

Based on the features, we employ the Nearest Neighbor algorithm [78] for pesticide detection. This straightforward classification can identify the closest match within our feature set for any new test sample based on its proximity, accurately and promptly ascertaining pesticide identities.

4 IMPLEMENTATION

Electrochemical Tag Setup: Our *Hornbill* tag is designed using a flexible PI substrate configured into a two-layer PCB, measuring 34mm×45mm, weighing 1.62 grams, and having a thin profile of 0.11mm (Fig. 13). The MSP430FR2433 (126 μ A/MHz, 15KB FRAM, 4KB SRAM) is selected as the microcontroller of our tag. The transducer circuit includes passive components like amplifiers, resistors, and capacitors, featuring an ultra-low power AD8659 operational amplifier (22 μ A max) for the potentiostat, which operates within a 0.4–0.9V range at 10mV/s. A charge pump using the ICL7660N (65 μ A max) serves as the negative voltage regulator. The NFC antenna, a three-loop rectangular design (44mm×33mm), enhances inductive coupling and saves space. For communication, we use the cost-effective NT3H2211 chip (1.15\$) with 2KB EEPROM and 106kbit/s rate, supporting the ISO14443A protocol, sufficient for pesticide detection.



Figure 13: Material electrodes, integrated circuit and real-world deployment of Hornbill system.

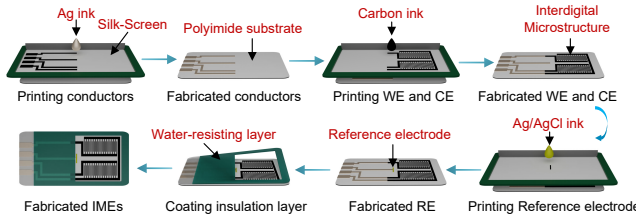


Figure 14: The fabrication workflow of system IMEs.

Smartphone Receiver Setup: To demonstrate the universality of *Hornbill*, we use an NFC-enabled smartphone (MI 9) as the tag reader, as shown in Fig. 13. We develop a mobile app for the smartphone to receive electrochemical I-V curves transmitted from the tag. The app employs the NFC API to engage the device’s magnetometer for tag detection. Upon identifying an NFC tag, it automatically transitions to the detection interface, ensuring continuous tag power. Once the electrochemical analysis concludes (*about 1 minute*), the tag stores the measurement data on the NFC chip, ready for transfer during the next connection.

Fabrication of Microelectrode: Fig. 14 details the workflow for crafting our interdigitated microelectrodes. We choose screen printing as a cost-effective method to produce our IMEs. First, we shape a three-layer silkscreen to match the different parts of the electrode structure. Then we use Polyimide as the substrate, placing it beneath the first layer to print conductors. Shifting to the second silkscreen, we create the WE and CE by printing carbon ink. Following this, the RE is printed using Ag/AgCl ink. Finally, a waterproof layer is used for encapsulation to enhance durability.

Materials Setup: All materials used in our systems are purchased from Sigma Aldrich [74] and Macklin [54] biochemical company. We employ physical adsorption to modify biological receptors. 10mg ZIF-8 powder is prepared into a dispersion with deionized water, and 10 μ L of this dispersion is applied to the surface of the working electrode. After drying, 10 μ L CS solution with a concentration of 0.5mg/mL and 10 μ L cholinesterase **B** solution with a concentration of 4mg/mL are added to its surface, respectively. The modified electrode is then left to dry on a heating platform at 25°C.

Table 1: 9 pesticides in our evaluation.

Pesticide Name	Target Crops	Purpose	Regions
Methyl-parathion	Cotton, Soybean	Insecticide	Africa
Chlorpyrifos	Apple	Insecticide	Global
Dimethoate	Rice	Insecticide	Asia, Europe
Trichlorfon	Soybean, Citrus, Tea	Insecticide	Africa
Profenofos	Cabbage	Insecticide	Africa
Acephate	Corn	Insecticide	America
Glyphosate	Apple, Citrus, Pear	Herbicide	Global
Anilofos	Rice	Herbicide	Asia
Iprobenfos	Rice	Fungicide	Asia

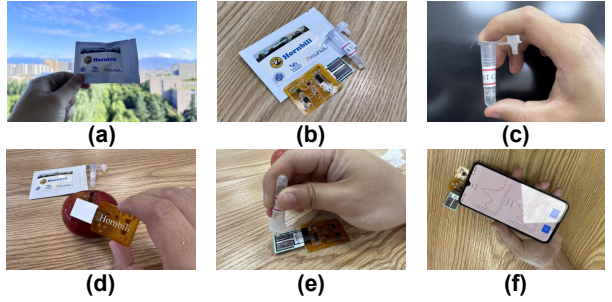


Figure 15: Future system integration: An examples of daily life applications.

As for enzyme substrate **A**, we choose acetylthiocholine iodide (ATCI) for its long shelf life. A 20 μ L dose at 2mmol/L concentration on the electrode is adequate for testing.

Pesticides: As indicated in Tab. 1, we pick 9 organophosphorus pesticides (OPs) that are the most extensively utilized globally [72] to evaluate the performance of *Hornbill*. For each pesticide, we diluted it into 5 concentration gradients ranging from 10⁻⁷-10⁻¹⁵mol/L, reducing it by 100 \times each time. The reason for selecting this concentration range is based on the maximum residue levels (MRLs=0.01mg/kg \approx 10⁻⁹mol/L) of pesticides permitted by the WHO’s Codex Alimentarius [26]. Hence, we use this concentration as a reference, covering both lower and higher levels to study below-MRL effects and those above MRLs.

Potential Future Application of Hornbill: Our *Hornbill* consists of three main components: the NFC tag, the interdigitated microelectrode with a biological receptor (enzyme), and the ATCI solution. These components can be conveniently packaged in a lightweight and portable pouch for future applications (Fig. 15(a-b)). To detect pesticides, the biological receptors on the tag must come into direct contact with fruits or vegetables that have pesticide residues. Following this, the ATCI solution, which reacts with the enzymes on our tag, is added (Fig. 15(d)). The pesticide influences this reaction, which is then detected by the three-electrode sensor. The incorporation of the ATCI solution does not necessarily require human intervention, as shown in Fig. 15(c), the solution can be prepackaged in plastic droppers. When measuring pesticides, users only need to add a quantified

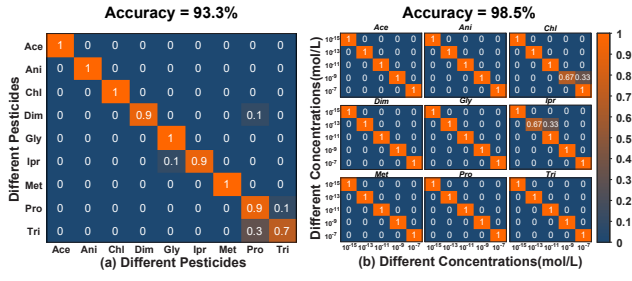


Figure 16: Detection performance for 9 pesticides.

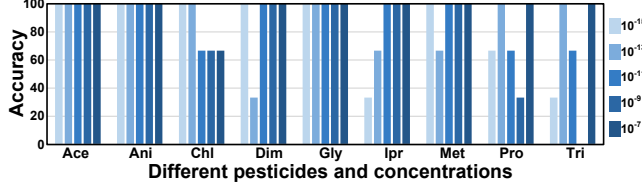


Figure 17: Performance in simultaneously classifying pesticide and concentrations.

amount (3-4 drops) of the ATCI solution onto the tag using the dropper (Fig. 15(e)) and use an NFC-enabled phone to approach the tag. Open our app and click the "Start Measurement" button to begin the measurement process (Fig. 15(f)).

5 EVALUATION

5.1 Performance of Pesticide Sensing

Experimental Setting. We first evaluate the pesticide sensing accuracy of *Hornbill*. For each experiment, we take $20\mu\text{l}$ of pesticide, drop it onto the surface of the IME, and leave it for 5 minutes to allow full interaction between the pesticide and cholinesterase **B**. Then, we add $20\mu\text{l}$ of the substrate ATCI and start the measurement by activating the smartphone's NFC function. For each concentration, we take three measurements, each lasting one minute.

Accuracy of Multi-pesticide Detection. Figure 16(a) shows the confusion matrix for the 9 pesticides in *Hornbill*. As can be seen, in most cases, *Hornbill* can accurately distinguish different types of pesticides—the average detection accuracy of the system reaches 93.3%. However, we observe that for a very small number of pesticides, *Trichlorfon*, the system's detection accuracy slightly decreases to 70%. This is due to the similar effects of this pesticide on enzymes compared to Pesticide *Profenofos*, leading to closely related dual enzyme features. Considering an increase in sample size or the use of more sophisticated feature extraction methods, such as deep learning, can address this issue.

Accuracy of Concentration Detection. Besides its classification tasks, the system is adept at analyzing pesticide concentrations. Figure 16(b) shows the concentration detection performance of the system under nine pesticides. In the figure, we can see that, with the pesticide type specified,

Table 2: Comparison with existing methods.

Ref.	Broad Spectrum	Electrode	Power Supply	Sensitivity (mol/L)
Work [87]	✗ One pesticide	3D SPE	Cable	1×10^{-4} to 1×10^{-5}
Work [73]	✓ Three pesticides	SPE	Battery	1×10^{-8} to 1×10^{-10}
Work [12]	✗ One pesticide	SPE	Battery	1×10^{-10} to 1×10^{-11}
Ours	✓ Nine pesticides	IME	NFC	1×10^{-7} to 1×10^{-15}

Table 3: Analysis of power consumption between *Hornbill* and existing systems

Systems	MCU	ADC/DAC	Sensor	Comm	Total Power
Apollo [85]	10.11 mW	7.2 mW	5.8 mW	0.18 mW	23.29 mW
iMED [59]	2500 mW	1800 mW	16 mW	924 mW	5240 mW
PalmSens [36]	—	—	—	—	650 mW
Wi-Fi-Based System [6]	2.29 mW	7.59 mW	1452 mW	950.4 mW	961.73 mW
Bluetooth-Based System [25]	82.5 mW	6.53 mW	15.18 mW	132 mW	236.21 mW
Our System	0.42 mW	3.98 mW	0.24 mW	0.79 mW	5.43 mW

the system achieves an average detection rate of 98.5% for pesticide concentrations, with only two out of 135 data sets incorrectly identifying the concentration levels. The results illustrate that the system is capable not only of qualitative pesticide identification but also of achieving commendable accuracy in quantitative pesticide analysis.

Simultaneously Classifying Types and Concentrations. In this experiment, we verify the performance of *Hornbill* when measuring both pesticide concentration and type. We can see from Fig. 17 that: Our system achieves an average recognition accuracy of 81%. Notably, it accurately identified both the type and concentration of three pesticides (*Acephate (Ace)*, *Glyphosate (Gly)*, and *Anilofos (Ani)*). This underscores the system's potential in qualitative and quantitative analysis of multiple pesticides simultaneously.

5.2 Comparison with Existing Methods

Compared with Existing Electrochemical Detectors. We begin by comparing our system's effectiveness with the latest developments in electrochemical methods for detecting pesticides. Through detailed statistical examination of findings from various studies, outlined in Tab. 2, we gather comprehensive insights. The analysis reveals that our method not only meets but surpasses existing standards, notably enhancing sensitivity and diversity in pesticide detection.

Compared with Commercial SPE. Additionally, we compare the system's the sensitivity with commercial sensors. Specifically, we compare our system with two commonly used commercial screen printing electrodes, Metrohm C110 (SPE1) [60] and MicruX S1PE (SPE2) [24], by applying equal volumes and concentrations of AChE ($10\mu\text{l}, 4\text{mg/mL}$) and *glyphosate* ($10\mu\text{l}, 10^{-15}\text{mol/L}$) on each of the three devices. We use an electrochemical workstation to continuously capture a peak current of 0.7V for 10s. Fig. 18 shows that our system achieves a peak average current of $2\times$ as high within this timeframe compared to two other commercial electrodes.

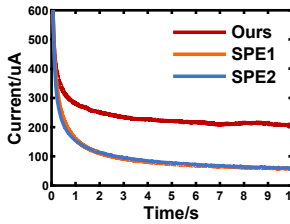


Figure 18: Electrode sensitivity comparison.

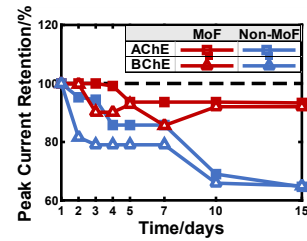


Figure 19: Durability of the system.

This result underscores the effectiveness of our electrode design in significantly enhancing the detection sensitivity for low-concentration pesticides.

5.3 Power Consumption

We conduct a detailed power consumption evaluation of our system and compare it with similar electrochemical systems recently published. The comparison is summarized in the Tab. 3. The power consumption measurements for *Hornbill* tag are obtained by the Monsoon Power Monitor AAA10F, a precision instrument designed for power profiling. Our system demonstrates superior power efficiency, with a total consumption of just 5.43 mW, the lowest among compared systems. It excels in minimizing power use across all components, especially in ADC/DAC and sensor functions. In contrast, systems like iMED [59] and PalmSens [36] show significantly higher power consumption. This efficiency makes our system a strong candidate for low-power applications.

5.4 Performance under Different factors

We evaluate the impact of several practical factors that are related to the applicability of *Hornbill* in practice.

Durability. The testing for durability is conducted across a range of room temperatures (15–25°C). We record the electrochemical curves of a total of 30 electrodes over 15 days, reflecting the system’s durability by tracking the retention of Faraday current peaks. The retention rate is the ratio of the peak current on the N_{th} day to the peak current on the first day. From Fig. 19, we can see that the nanostructured coating significantly contributed to the sensor’s durability, protecting the electrode surface from physical damage. Even after exposure to room temperature conditions for 15 days, the sensor retains more than 93.3% of its original performance, marking a 30% improvement in peak retention compared to unprotected enzyme electrodes.

Impact of Different Devices. Different devices have varying NFC antennas. To validate the robustness of our system across different devices, we use six different models of mobile devices (P1: Xiaomi9, P2: Redmi K30S Ultra, P3: OPPO Reno3 Pro, P4: Redmi K60, P5: Vivo X60 Pro, and P6: Redmi K40 Pro) to power *Hornbill* and measure the electrochemical response. The measurement results are shown in Fig. 20. We

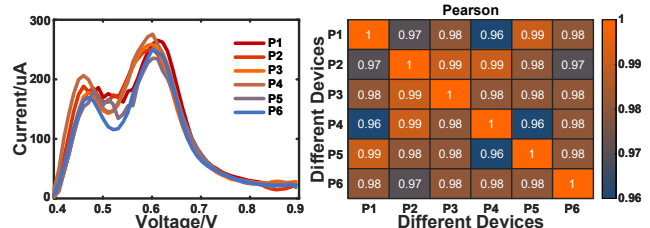


Figure 20: Left, electrochemical curves by 6 different phones. Right, the Pearson similarity of each other.

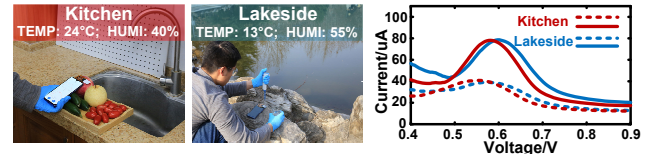


Figure 21: Pesticide detection performance in different environments (Dashed line: After pesticide addition).

can see that different devices measuring the same NFC tag have similar electrochemical curves and obtain high Pearson similarity, which is sufficient to demonstrate the device robustness of our system.

Impact of Different Environment. Fig. 21 presents the experimental setup and corresponding electrochemical responses for pesticide detection in two distinct environments: a kitchen (24°C, 40% humidity) and lakeside (13°C, 55% humidity). In both environments, our system exhibits a clear redox peak around 0.6V, confirming its capability to detect pesticides. Despite significant differences in temperature and humidity between the two environments, the current response measured by our tag hardly change, indicating the robustness of *Hornbill* across different environments.

6 RELATED WORK

Pesticide Chromatography Analysis. Chromatography-based methods, such as liquid chromatography [35], gas chromatography [83], and liquid/gas chromatography-mass spectrometry [56], are highly accurate for detecting small amounts of pesticides in environmental samples and are vital for environmental monitoring. Yet, their effective use demands considerable expertise and precise calibration, alongside notable equipment costs and maintenance expenses, making them unsuitable for scenarios demanding rapid on-site testing. For quick on-site detection, affordable options like color cards and test papers using spectrophotometry [32] and Raman spectroscopy [82] are available, but their performance declines under adverse conditions such as light exposure, temperature changes, or low concentrations.

Electrochemical Analysis for Pesticide Detection. Significant efforts have been made to use electrochemical analysis for pesticide sensing. For example, electrochemical biosensors [14, 19, 81] detect pesticides through electrical changes

caused by reactions between pesticides and biological receptors like cholinesterases [7], aptamers [63], and antibodies [67]. Nanomaterials are also used to mimic biological receptors, enhancing sensitivity and robustness. For example, 2D Ni metal-organic frameworks assist peroxidase enzymes in detecting hydrogen peroxide [13], and ceric dioxide nanoparticles mimic oxidase enzymes to identify chlorpyrifos [15]. The main focus of research in these directions has been designing diverse receptors or nanomaterials that are sensitive to applied pesticide molecules. They are powerful tools for *in situ* analysis due to their fast response, time-saving processes, and user-friendly procedures.

However, the substantial power requirements of electrochemical methods necessitate the use of external batteries or wired connections for pesticide detection. Additionally, their limited detection range, combined with concerns about environmental robustness and material durability, restricts the widespread use of electrochemical biosensors. In contrast, our *Hornbill* leverages advances in electrochemistry, materials science, and NFC backscatter technology to introduce a portable, cost-effective, and battery-free electrochemical bio-tag for multi-pesticide detection.

RF-based Sensing System. In addition to the methods mentioned, RF-based sensing techniques that modify sensor impedance [48, 66], inductance [16], and capacitance [47, 77] to influence antenna signal reception offer novel approaches. For example, Liu *et al.* [52] demonstrate biomarker identification in biological fluids by adjusting the capacitance in the antenna's RLC circuit, showcasing potential for precise, non-invasive diagnostics. However, these methods often need to utilize network analyzers or RFID readers to measure changes in the RLC of sensing tags, which is far from a working system on popular commercial devices (e.g., a smartphone) or only perform a feasibility study of sensing within a very high concentration range (e.g., 100–700 μM) which is far from useful for real-world pesticide sensing.

In contrast, our system requires only NFC-equipped smartphones for seamless sensor interaction, providing accurate pesticide measurements. This simplified approach enables users to effortlessly perform pesticide testing anywhere and at any time, making large-scale deployment possible.

7 CONCLUSION

In this work, we present *Hornbill*, a wireless and battery-free electrochemical NFC tag that can realize portable, precise, and touchless multi-pesticide detection. Our comprehensive design and experimental evaluation show that *Hornbill* not only enables sensing the molecular-level changes in pesticides but also sparks the inspiration for other novel applications such as implantable medical devices.

ACKNOWLEDGEMENTS

Thanks to the anonymous shepherd and reviewers for their valuable comments. This work is supported by National Natural Science Foundation of China under Grants (62372372, 62272388, 62372374) and the Shaanxi International Science and Technology Cooperation Program (2024GH-ZDXM-50, 2024GH-YBXM-07, 2024GH-ZDXM-49).

REFERENCES

- [1] Mohammad Mahdi Ahmadi and Graham A Jullien. 2008. Current-mirror-based potentiostats for three-electrode amperometric electrochemical sensors. *IEEE Transactions on Circuits and Systems I: Regular Papers* 56, 7 (2008), 1339–1348.
- [2] Jun-ichi Anzai. 2009. Biosensors for the detection of OP nerve agents. In *Handbook of toxicology of chemical warfare agents*. Elsevier, 837–846.
- [3] Sunil Aryal and Lok Nath Aryal. 2023. Pesticide Residue and Food Safety: Retrospection and Prospects. In *Emerging Solutions in Sustainable Food and Nutrition Security*. Springer, 183–210.
- [4] Samir Banerjee and M.V.D.Van Der Heijden. 2023. Soil microbiomes and one health. *Nature Reviews Microbiology* 21, 1 (2023), 6–20.
- [5] Allen J Bard, Larry R Faulkner, and Henry S White. 2022. *Electrochemical methods: fundamentals and applications*. John Wiley & Sons.
- [6] Valentina Bianchi, Andrea Boni, Simone Fortunati, Marco Giannetto, Maria Careri, and Ilaria De Munari. 2019. A Wi-Fi cloud-based portable potentiostat for electrochemical biosensors. *IEEE Transactions on Instrumentation and Measurement* 69, 6 (2019), 3232–3240.
- [7] Sehrish Bilal, M Mudassir Hassan, Muhammad Fayyaz ur Rehman, Muhammad Nasir, Amtul Jamil Sami, and Akhtar Hayat. 2021. An insect acetylcholinesterase biosensor utilizing WO₃/g-C₃N₄ nanocomposite modified pencil graphite electrode for phosmet detection in stored grains. *Food Chemistry* 346 (2021), 128894.
- [8] Aaron Blair, Beate Ritz, Catharina Wesseling, and Laura Beane Freeman. 2015. Pesticides and human health. , 81–82 pages.
- [9] Carsten A Brühl and Johann G Zaller. 2019. Biodiversity decline as a consequence of an inappropriate environmental risk assessment of pesticides. *Frontiers in Environmental Science* (2019), 177.
- [10] RW Byard and M Carli. 1998. Temporal stability of acetylcholinesterase staining in colonic and rectal neural tissue. *Pediatric surgery international* 13 (1998), 29–31.
- [11] Zhonglin Cao, Ping Chen, Zhong Ma, Sheng Li, Xingxun Gao, Rui-xin Wu, Lijia Pan, and Yi Shi. 2019. Near-field communication sensors. *Sensors* 19, 18 (2019), 3947.
- [12] Satyapal Chaudhary, Ashish Mani, Lalit M Bharadwaj, Tinku Basu, et al. 2022. A mobile app integrated portable Electrochemical sensor for rapid detection of Organophosphate pesticides in vegetable extract. *Materials Letters* 309 (2022), 131319.
- [13] Jingyuan Chen, Yun Shu, Huilei Li, Qin Xu, and Xiaoya Hu. 2018. Nickel metal-organic framework 2D nanosheets with enhanced peroxidase nanozyme activity for colorimetric detection of H₂O₂. *Talanta* 189 (2018), 254–261.
- [14] Shulin Chen, Tzu-Li Liu, Yizhen Jia, and Jinghua Li. 2023. Recent Advances in Bio-Integrated Electrochemical Sensors for Neuroengineering. *Fundamental Research* (2023).
- [15] Zhengyi Chen, Yanan Wang, Yuting Mo, Xiaoyun Long, Hao Zhao, Linjing Su, Zhenhua Duan, and Yuhao Xiong. 2020. ZIF-8 directed templating synthesis of CeO₂ nanoparticles and its oxidase-like activity for colorimetric detection. *Sensors and actuators B: chemical* 323 (2020), 128625.

- [16] Kevin P Cohen, William M Ladd, David M Beams, William S Sheers, Robert G Radwin, Willis J Tompkins, and John G Webster. 1997. Comparison of impedance and inductance ventilation sensors on adults during breathing, motion, and simulated airway obstruction. *IEEE Transactions on Biomedical Engineering* 44, 7 (1997), 555–566.
- [17] COMSOL. 2024. Electrochemistry Module User's Guide. <https://doc.comsol.com/6.2/doc/com.comsol.help.echem/ElectrochemistryModuleUsersGuide.pdf>
- [18] Wikipedia contributors. 2024. Standard electrode potential—Wikipedia, The Free Encyclopedia. [https://en.wikipedia.org/w/index.php?title=Standard_electrode_potential_\(data_page\)&oldid=1199472542](https://en.wikipedia.org/w/index.php?title=Standard_electrode_potential_(data_page)&oldid=1199472542)
- [19] Antonella Curulli. 2021. Electrochemical biosensors in food safety: Challenges and perspectives. *Molecules* 26, 10 (2021), 2940.
- [20] Donghui Dai, Zhenlin An, Qingrui Pan, and Lei Yang. 2023. Magcode: Nfc-enabled barcodes for nfc-disabled smartphones. In *Proceedings of the 29th Annual International Conference on Mobile Computing and Networking*. 1–14.
- [21] Analog Devices. 2023. AD5689R. https://www.analog.com/en/products/ad5689r.html?doc=AD5689R_5687R.pdf.
- [22] Yingjie Du, Xiaotong Jia, Le Zhong, Yi Jiao, Zhijin Zhang, Ziyuan Wang, Yuxiao Feng, Muhammad Bilal, Jiandong Cui, and Shiru Jia. 2022. Metal-organic frameworks with different dimensionalities: An ideal host platform for enzyme@ MOF composites. *Coordination Chemistry Reviews* 454 (2022), 214327.
- [23] Anitha R Dudhani and Shantha L Kosaraju. 2010. Bioadhesive chitosan nanoparticles: Preparation and characterization. *Carbohydrate polymers* 81, 2 (2010), 243–251.
- [24] MICRUX ECSENS. 2024. SINGLE ELECTRODES (S1PE). <https://www.micruxfluidic.com/en/>
- [25] Liang Fan, Jinhui Jeanne Huang, and Jianjun Liao. 2022. Competitive smartphone-based portable electrochemical aptasensor system based on an MXene/cDNA-MB probe for the determination of Microcystin-LR. *Sensors and Actuators B: Chemical* 369 (2022), 132164.
- [26] Oluwatoyin T Fatunsin, Aderonke O Oyeyiola, Muyideen O Moshood, Latifat M Akanbi, and Damilola E Fadahunsi. 2020. Dietary risk assessment of organophosphate and carbamate pesticide residues in commonly eaten food crops. *Scientific African* 8 (2020), e00442.
- [27] Dawei Feng, Tian-Fu Liu, Jie Su, Mathieu Bosch, Zhangwen Wei, Wei Wan, Daqiang Yuan, Ying-Pin Chen, Xuan Wang, Kecheng Wang, et al. 2015. Stable metal-organic frameworks containing single-molecule traps for enzyme encapsulation. *Nature communications* 6, 1 (2015), 5979.
- [28] Morgan Ferguson, Dhavan Sharma, David Ross, and Feng Zhao. 2019. A critical review of microelectrode arrays and strategies for improving neural interfaces. *Advanced healthcare materials* 8, 19 (2019), 1900558.
- [29] Song Gao, Jingwei Hou, Zeyu Deng, Tiesheng Wang, Sebastian Beyer, Ana Guilherme Buzanich, Joseph J Richardson, Aditya Rawal, Robert Seidel, Muhammad Yazid Zulkifli, et al. 2019. Improving the acidic stability of zeolitic imidazolate frameworks by biofunctional molecules. *Chem* 5, 6 (2019), 1597–1608.
- [30] Prateek Goyal, Pushpanjali Soppina, Superb K Misra, Eugenia Valsamis-Jones, Virupakshi Soppina, and Swaroop Chakraborty. 2022. Toxicological Impact and in Vivo Tracing of Rhodamine Functionalised ZIF-8 Nanoparticles. *Frontiers in toxicology* 4 (2022), 917749.
- [31] JingYi Han, Mingji Li, Hongji Li, Cuiping Li, Jianshan Ye, and Baohe Yang. 2020. Pt-poly (L-lactic acid) microelectrode-based microsensor for in situ glucose detection in sweat. *Biosensors and Bioelectronics* 170 (2020), 112675.
- [32] Dave Harshit, Kothari Charmy, and Patel Nrupesh. 2017. Organophosphorus pesticides determination by novel HPLC and spectrophotometric method. *Food chemistry* 230 (2017), 448–453.
- [33] Quanguo He, Bing Wang, Jing Liang, Jun Liu, Bo Liang, Guangli Li, Yaohang Long, Gongyou Zhang, and Hongmei Liu. 2023. Research on the construction of portable electrochemical sensors for environmental compounds quality monitoring. *Materials Today Advances* 17 (2023), 100340.
- [34] Henderi Henderi, Tri Wahyuningsih, and Efana Rahwanto. 2021. Comparison of Min-Max normalization and Z-Score Normalization in the K-nearest neighbor (kNN) Algorithm to Test the Accuracy of Types of Breast Cancer. *International Journal of Informatics and Information Systems* 4, 1 (2021), 13–20.
- [35] Elbert Hogendoorn and Piet van Zoonen. 2000. Recent and future developments of liquid chromatography in pesticide trace analysis. *Journal of Chromatography A* 892, 1-2 (2000), 435–453.
- [36] De Indruk. 2024. Palmsens. <https://www.palmsens.com/>
- [37] Paul C Jepson, Katie Murray, Oliver Bach, Maria A Bonilla, and Lars Neumeister. 2020. Selection of pesticides to reduce human and environmental health risks: a global guideline and minimum pesticides list. *The Lancet Planetary Health* 4, 2 (2020), e56–e63.
- [38] Wenli Jiao, Yanlin Li, Xiangdong Xi, Ju Wang, Dingyi Fang, and Xiaojiang Chen. 2023. BioScatter: Low-Power Sweat Sensing with Backscatter. In *Proceedings of the 21st Annual International Conference on Mobile Systems, Applications and Services*. 191–204.
- [39] Milan Jokanović. 2018. Neurotoxic effects of organophosphorus pesticides and possible association with neurodegenerative diseases in man: A review. *Toxicology* 410 (2018), 125–131.
- [40] Milan Jokanović, Patrik Oleksak, and Kamil Kuca. 2023. Multiple neurological effects associated with exposure to organophosphorus pesticides in man. *Toxicology* 484 (2023), 153407.
- [41] Hye Jin Kim, Woongsun Choi, Jinsik Kim, Jungkyu Choi, Nakwon Choi, and Kyo Seon Hwang. 2020. Highly sensitive three-dimensional interdigitated microelectrode biosensors embedded with porosity tunable hydrogel for detecting proteins. *Sensors and Actuators B: Chemical* 302 (2020), 127190.
- [42] Ki-Hyun Kim, Ehsanul Kabir, and Shamin Ara Jahan. 2017. Exposure to pesticides and the associated human health effects. *Science of the total environment* 575 (2017), 525–535.
- [43] G Kiran Kumar, Tarakanath Kobaku, Subham Sahoo, Bidyadhar Subudhi, Devaraj Elangovan, and Frede Blaabjerg. 2021. An Overview of Fully Integrated Switching Power Converters Based on Switched-Capacitor versus Inductive Approach and Their Advanced Control Aspects. *Energies* 14, 11 (2021), 3250.
- [44] Karnpimon Krorakai, Supannika Klangphukhiew, Sirinan Kulchat, and Rina Patramanon. 2021. Smartphone-based NFC potentiostat for wireless electrochemical sensing. *Applied Sciences* 11, 1 (2021), 392.
- [45] Sneha Kumari, Thomas S Howlett, Ryanne N Ehrman, Shailendra Koirala, Orikeda Trashi, Ikeda Trashi, Yalini H Wijesundara, and Jeremiah J Gassensmith. 2023. In vivo biocompatibility of ZIF-8 for slow release via intranasal administration. *Chemical Science* 14, 21 (2023), 5774–5782.
- [46] Poonam Lathiya and Jing Wang. 2021. Near-field communications (nfc) for wireless power transfer (wpt): An overview. *Wireless Power Transfer—Recent Development, Applications and New Perspectives* (2021).
- [47] Antonio Lazar, Martí Boada, Ramón Villarino, and David Girbau. 2019. Battery-less smart diaper based on NFC technology. *IEEE Sensors Journal* 19, 22 (2019), 10848–10858.
- [48] Liyao Li, Yaxiong Xie, Jie Xiong, Ziyu Hou, Yingchun Zhang, Qing We, Fuwei Wang, Dingyi Fang, and Xiaojiang Chen. 2022. SmartLens: sensing eye activities using zero-power contact lens. In *Proceedings of the 28th Annual International Conference on Mobile Computing And Networking*. 473–486.
- [49] Ruixia Li, Minghui Shang, Taotao Zhe, Mingyan Li, Feier Bai, Zhi-hao Xu, Tong Bu, Fan Li, and Li Wang. 2023. Sn/MoC@ NC hollow

- nanospheres as Schottky catalyst for highly sensitive electrochemical detection of methyl parathion. *Journal of Hazardous Materials* 447 (2023), 130777.
- [50] Tian Li, Xin Wang, Lean Zhou, Jingkun An, Junhui Li, Nan Li, Hongwen Sun, and Qixing Zhou. 2016. Bioelectrochemical sensor using living biofilm to in situ evaluate flocculant toxicity. *ACS Sensors* 1, 11 (2016), 1374–1379.
- [51] Truman S Light. 1972. Standard solution for redox potential measurements. *Analytical Chemistry* 44, 6 (1972), 1038–1039.
- [52] Tzu-Li Liu, Yan Dong, Shulin Chen, Jie Zhou, Zhenqiang Ma, and Jinghua Li. 2022. Battery-free, tuning circuit-inspired wireless sensor systems for detection of multiple biomarkers in bodily fluids. *Science Advances* 8, 27 (2022), eab07049.
- [53] J Ross Macdonald and Carl A Barlow Jr. 1962. Theory of double-layer differential Capacitance in electrolytes. *The Journal of Chemical Physics* 36, 11 (1962), 3062–3080.
- [54] Macklin. 2024. Macklin. <https://www.macklin.cn>
- [55] Amanda Mascarelli. 2013. Growing Up With Pesticides. *Science* 341, 6147 (2013), 740–741. <https://doi.org/10.1126/science.341.6147.740>
- [56] Ana Masiá, Cristina Blasco, and Yolanda Picó. 2014. Last trends in pesticide residue determination by liquid chromatography-mass spectrometry. *Trends in Environmental Analytical Chemistry* 2 (2014), 11–24.
- [57] Jarosław Mazuryk, Katarzyna Klepacka, Włodzimierz Kutner, and Piyush Sindhu Sharma. 2023. Glyphosate separating and sensing for precision agriculture and environmental protection in the era of smart materials. *Environmental Science & Technology* 57, 27 (2023), 9898–9924.
- [58] Eve McGlynn, Vahid Nabaei, Elisa Ren, Gabriel Galeote-Checa, Rupam Das, Giulia Curia, and Hadi Heidari. 2021. The future of neuroscience: flexible and wireless implantable neural electronics. *Advanced Science* 8, 10 (2021), 2002693.
- [59] Conan Mercer, Richard Bennett, Peter Ó Conghaile, James F Rusling, and Dónal Leech. 2019. Glucose biosensor based on open-source wireless microfluidic potentiostat. *Sensors and Actuators B: Chemical* 290 (2019), 616–624.
- [60] Metrohm. 2024. Screen printed carbon electrodes C110. https://www.metrohm.com/zh_tw/products/c11/c110.html
- [61] Gaetano Palumbo and Domenico Pappalardo. 2010. Charge pump circuits: An overview on design strategies and topologies. *IEEE Circuits and Systems Magazine* 10, 1 (2010), 31–45.
- [62] Xiang Qi, Panpan Liu, Peng Liang, Wen Hao, Meng Li, Qingchen Li, Yuexi Zhou, and Xia Huang. 2020. Biofilm's morphology design for high sensitivity of bioelectrochemical sensor: An experimental and modeling study. *Science of the Total Environment* 729 (2020), 138908.
- [63] Abd-Elgawad Radi et al. 2011. Electrochemical aptamer-based biosensors: recent advances and perspectives. *International journal of electrochemistry* 2011 (2011).
- [64] Aman Raj, Anamika Dubey, Muneer Ahmad Malla, and Ashwani Kumar. 2023. Pesticide pestilence: Global scenario and recent advances in detection and degradation methods. *Journal of Environmental Management* 338 (2023), 117680.
- [65] Umamaheswari Rajaji, Sathishkumar Chinnapaiyan, Shen-Ming Chen, Mani Govindasamy, Jose Ilton de Oliveira Filho, Walaa Khushaim, and Veerappan Mani. 2021. Design and fabrication of yttrium ferrite garnet-embedded graphitic carbon nitride: a sensitive electrocatalyst for smartphone-enabled point-of-care pesticide (mesotriione) analysis in food samples. *ACS Applied Materials & Interfaces* 13, 21 (2021), 24865–24876.
- [66] Rasha B Rashid, Alwan M Alwan, and Mohammed S Mohammed. 2023. Improved Difenconazole pesticide detection limit via double-sided porous silicon layers' electrical sensor. *Materials Chemistry and Physics* 293 (2023), 126898.
- [67] Francesco Ricci, Gianluca Adornetto, and Giuseppe Palleschi. 2012. A review of experimental aspects of electrochemical immunosensors. *Electrochimica Acta* 84 (2012), 74–83.
- [68] Michael Roland. 2012. Software card emulation in NFC-enabled mobile phones: great advantage or security nightmare. In *Fourth international workshop on security and privacy in spontaneous interaction and mobile phone use*. 1–6.
- [69] Niina J Ronkainen, H Brian Halsall, and William R Heineman. 2010. Electrochemical biosensors. *Chemical Society Reviews* 39, 5 (2010), 1747–1763.
- [70] Gerhard Schrom, P Hazucha, Fabrice Paillet, DJ Rennie, ST Moon, DS Gardner, T Kamik, P Sun, TT Nguyen, MJ Hill, et al. 2007. A 100MHz eight-phase buck converter delivering 12A in 25mm² using air-core inductors. In *APEC 07-Twenty-Second Annual IEEE Applied Power Electronics Conference and Exposition*. IEEE, 727–730.
- [71] NXP Semiconductors. 2023. NTAG I2C plus: NFC Forum T2T with I2C interface, password protection and energy harvesting. https://www.nxp.com/docs/en/data-sheet/NT3H2111_2211.pdf.
- [72] Anket Sharma, Vinod Kumar, Babar Shahzad, Mohsin Tanveer, Gagan Preet Singh Sidhu, Neha Handa, Sukhmeen Kaur Kohli, Poonam Yadav, Aditi Shreeya Bali, Ripu Daman Parihar, et al. 2019. Worldwide pesticide usage and its impacts on ecosystem. *SN Applied Sciences* 1 (2019), 1–16.
- [73] Qianwei Shi, Yuanjie Teng, Yuchao Zhang, and Wenhan Liu. 2018. Rapid detection of organophosphorus pesticide residue on Prussian blue modified dual-channel screen-printed electrodes combining with portable potentiostat. *Chinese Chemical Letters* 29, 9 (2018), 1379–1382.
- [74] Sigma-Aldrich. 2024. Sigma-Aldrich. <https://www.sigmapellichi.com>
- [75] Vera Silva, Hans GJ Mol, Paul Zomer, Marc Tienstra, Coen J Ritsema, and Violette Geissen. 2019. Pesticide residues in European agricultural soils—A hidden reality unfolded. *Science of the Total Environment* 653 (2019), 1532–1545.
- [76] Donghui Song, Lulu Lei, Tian Tian, Xiaoyu Yang, Luwei Wang, Yongxin Li, and Hui Huang. 2023. A novel strategy for identification of pesticides in different categories by concentration-independent model based on a nanozyme with multienzyme-like activities. *Biosensors and Bioelectronics* (2023), 115458.
- [77] Nicolas R Tanguy, Benjamin Wiltshire, Mohammad Arjmand, Mohammad H Zarifi, and Ning Yan. 2020. Highly sensitive and contactless ammonia detection based on nanocomposites of phosphate-functionalized reduced graphene oxide/polyaniline immobilized on microstrip resonators. *ACS applied materials & interfaces* 12, 8 (2020), 9746–9754.
- [78] Kashvi Taunk, Sanjukta De, Srishti Verma, and Aleena Swetapadma. 2019. A brief review of nearest neighbor algorithm for learning and classification. In *2019 international conference on intelligent computing and control systems (ICCS)*. IEEE, 1255–1260.
- [79] Christopher John Topping, Annette Aldrich, and Philippe Berny. 2020. Overhaul environmental risk assessment for pesticides. *Science* 367, 6476 (2020), 360–363.
- [80] Graziella L Turdean, Ionel Catalin Popescu, Liviu Oniciu, and Daniel R Thevenot. 2002. Sensitive detection of organophosphorus pesticides using a needle type amperometric acetylcholinesterase-based bioelectrode. Thiocholine electrochemistry and immobilised enzyme inhibition. *Journal of enzyme inhibition and medicinal chemistry* 17, 2 (2002), 107–115.
- [81] Reddicherla Umapathi, Seyed Majid Ghoreishian, Sonam Sonwal, Gokana Mohana Rani, and Yun Suk Huh. 2022. Portable electrochemical sensing methodologies for on-site detection of pesticide residues in fruits and vegetables. *Coordination Chemistry Reviews* 453 (2022), 214305.

- [82] Su-Yan Wang, Xin-Chi Shi, Gui-Yang Zhu, Yun-Jiao Zhang, Da-Yong Jin, Yi-Dong Zhou, Feng-Quan Liu, and Pedro Laborda. 2021. Application of surface-enhanced Raman spectroscopy using silver and gold nanoparticles for the detection of pesticides in fruit and fruit juice. *Trends in Food Science & Technology* 116 (2021), 583–602.
- [83] Jon W Wong, Kai Zhang, Katherine Tech, Douglas G Hayward, Carolyn M Makovi, Alexander J Krynnitsky, Frank J Schenck, Kaushik Banerjee, Soma Dasgupta, and Don Brown. 2010. Multiresidue pesticide analysis in fresh produce by capillary gas chromatography-mass spectrometry/selective ion monitoring (GC-MS/SIM) and- tandem mass spectrometry (GC-MS/MS). *Journal of Agricultural and Food Chemistry* 58, 10 (2010), 5868–5883.
- [84] Huizhong Ye, Chi-Jung Lee, Te-Yen Wu, Xing-Dong Yang, Bing-Yu Chen, and Rong-Hao Liang. 2022. Body-centric NFC: Body-centric interaction with NFC devices through near-field enabled clothing. In *Designing Interactive Systems Conference*. 1626–1639.
- [85] Lonzh Yuan, Can Xiong, Si Chen, and Wei Gong. 2021. Embracing self-powered wireless wearables for smart healthcare. In *2021 IEEE International Conference on Pervasive Computing and Communications (PerCom)*. IEEE, 1–7.
- [86] Yana Zeng, Donghui Liao, Xiangyang Kong, Qianying Huang, Muqi Zhong, Jianqiang Liu, Alireza Nezamzadeh-Ejhieh, Ying Pan, and Hailiang Song. 2023. Current status and prospect of ZIF-based materials for breast cancer treatment. *Colloids and Surfaces B: Biointerfaces* 232 (2023), 113612.
- [87] Fengnian Zhao, Jianwei He, Xunjia Li, Yunpeng Bai, Yibin Ying, and Jianfeng Ping. 2020. Smart plant-wearable biosensor for in-situ pesticide analysis. *Biosensors and Bioelectronics* 170 (2020), 112636.
- [88] Renjie Zhao, Purui Wang, Yunfei Ma, Pengyu Zhang, Hongqiang Harry Liu, Xianshang Lin, Xinyu Zhang, Chenren Xu, and Ming Zhang. 2020. Nfc+ breaking nfc networking limits through resonance engineering. In *Proceedings of the Annual conference of the ACM Special Interest Group on Data Communication on the applications, technologies, architectures, and protocols for computer communication*. 694–707.